



# Optimizing the exponential sine sweep (ESS) signal for in situ measurements on noise barriers

Massimo Garai

Department of Industrial Engineering, University of Bologna, Bologna, Italy.

Paolo Guidorzi

Department of Industrial Engineering, University of Bologna, Bologna, Italy.

## Summary

The measurement of sound reflection and airborne sound insulation of noise barriers is based on the acquisition of impulse responses by means of digital devices. The most widely used methods employ MLS (Maximum Length Sequence) or ESS (Exponential Sine Sweep) as test signals. The theory behind MLS generation and use is well developed and does not involve computational problems. That is why in CEN/TS 1793-5:2003 an MLS signal is recommended. During the European project QUIESST also an ESS signal was applied. The ESS signal has some advantages over MLS, such as a better signal to noise ratio (SNR) and a robust non-linearity rejection. Anyway, the generation of an ESS signal and the subsequent analysis of impulse responses involve some problems whose solutions are not yet common practice. These solutions are discussed here and practical application examples are presented.

PACS no. 43.58.Gn, 43.58.Kr, 43.55.Mc, 43.60.Ac

## 1. Introduction

The use of a MLS (Maximum Length Sequence) signal for measuring impulse responses is well established [1], [2], [3]. The sine sweep signal is also widely used [4]. In particular, the ESS (Exponential Sine Sweep) signal has gained considerable interest since Farina introduced it in 2000 [5] and refined it in 2007 [6]. It has some advantages over MLS and some drawbacks. The main advantage of the ESS method is the separation of the linear part of the measured impulse response of the system from most part of the harmonic distortion, even if recent works have shown that some amount of odd orders distortion still remains, as formally proved in 2011 Torras et al. [7]. The partial contamination of nonlinear distortion to the causal part of the impulse response was earlier found by Cirik in 2007 [8] and confirmed by other authors such as Kemp et al. in 2011 [9] or Dietrich et al. in 2013 [10] or Gusky et al. in 2014 [11]. The separation of the most part of distortion from the linear part permits to have a much better signal to noise ratio (SNR) than with MLS, because the impulse response is free from the spurious peaks distributed on the time axis typically caused by distortion when using MLS. Using ESS instead, the impulse response is recovered by means of an aperiodic linear convolution, avoiding the time-

aliasing problem of MLS. Moreover, employing an ESS measurement signal allows to easily describe the nonlinearities of the measured system by means of the Volterra model [12] and its simplified implementation (Diagonal Volterra model). The crest factor of about 3 dB of the ESS can be exploited performing high power measurements in (steady) noisy conditions. Typically, in similar conditions the ESS has a dynamic range of about 15 dB higher than MLS.

## 2. Effect of impulsive background noise

Whereas stationary background noise can be somehow rejected and compensated in different ways for both MLS and ESS methods [11], impulsive noises can contaminate the data sampled using an ESS signal, causing spurious effects on the deconvolved impulse response in form of a frequency decreasing sweep [4], [6]. Figure 1 (a) shows an example of measurement taken inside a concert hall in presence of extraneous background activity causing impulsive noise. This problem may be even worse when measuring outdoors, e.g. in order to characterize a noise barrier according to CEN/TS 1793-5 and/or EN 1793-6 on a construction site - where impulsive noise is usual - or close to a bridge with structural joints or along a railway with non-continuous rails [14], [15], [16],

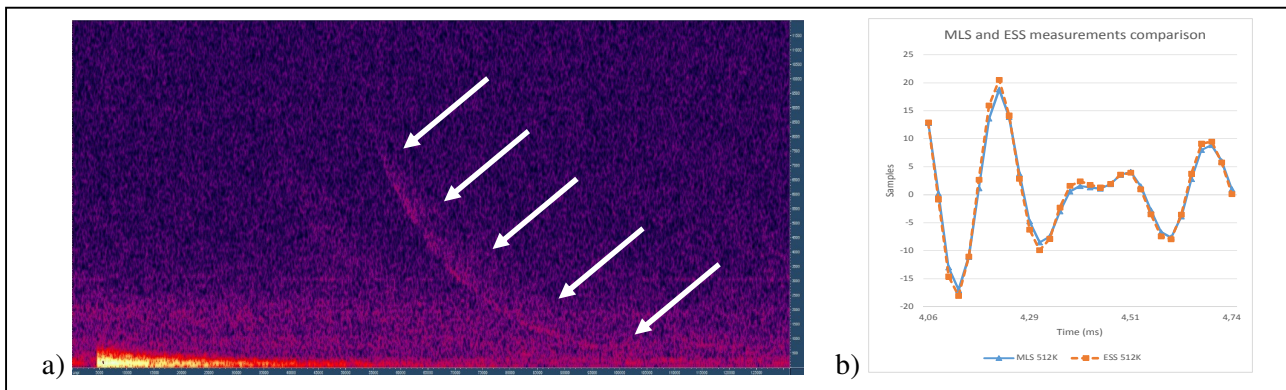


Figure 1. Spectrogram of an impulse response taken inside a concert hall. A frequency decreasing sweep occurs (see the arrows) due to an impulsive noise during the measurement.

[17]. Farina in [6] proposed a possible workaround for correcting a measurement corrupted by an impulsive noise, consisting in rejecting with a narrow-band filter the portion of sampled ESS corrupted by the noise, tuning the filter at the same frequency of the ESS at the disturbance instant. But this procedure can be applied only if the sampled ESS is available and not when a measurement system gives in output directly the deconvolved impulse response. Also, depending on the kind and duration of the disturbance, the manual correction of the ESS may not be possible.

### 3. Phase controlled ESS

Using MLS, the reconstruction by means of Fast Hadamard Transform of the measured impulse response provides ideal results; if the device under test has an unitary transfer function (performing a digital loopback measurement) the obtained impulse response is an ideal Dirac delta function, having therefore a perfectly flat frequency response. The generation and optimization of the ESS signal is more tricky because the employed signal, unlike the MLS, does not cover the entire frequency analysis range (ideally infinite, but in case of measurement using a soundcard the whole range goes from DC to Nyquist frequency). For this reason, the “best” obtainable impulse response in this case is no more an unitary pulse and some ringing around the main peak and some ripple in the corresponding frequency response appear. The phase-controlled ESS signal employed in this work was proposed by Vetter and di Rosario [13], but actually the idea of a phase-controlled swept (also

known as synchronized swept sine) was introduced by Novak [12] in order to better separate the several orders of harmonic distortion and compute correctly the Volterra kernels. By so doing, also the recovered linear impulse response will have the best possible “shape”. The ESS definition by Vetter and di Rosario, implemented here implicitly follows the Novak formulation, with some enhancements. The ESS signal is defined as:

$$x[n] = \sin \left[ \left( \frac{\pi}{2^P} \right)^L \frac{n}{\ln(2^P)} e^{\frac{n}{N} \ln(2^P)} \right] \quad (1)$$

$$\left( \frac{\pi}{2^P} \right) \cdot L = M \cdot \pi \cdot 2 \cdot \ln(2^P) \quad (2)$$

where  $n$  is the index of the generated sequence,  $P$  is an integer number of octaves,  $L$  the theoretical length of the ESS (floating point value),  $N$  the actual ESS length (equal to  $L$  rounded to integer) and  $M$  a positive non-zero integer. In this formulation, the signal contains exactly  $P$  octaves, the stop frequency of the sweep is always fixed at the Nyquist frequency and the start frequency is then  $\pi/2^P$  radians. Once the number of octaves and the maximum length of the sweep are chosen,  $L$ , and then  $N$ , are computed from equation 2. A very small phase mismatch error remains because of the rounding of  $L$ . The time-reversed signal, used for the deconvolution, is then:

$$x^{-1}[n] = x[N - n] \cdot \left( \frac{P}{2^N} \right)^{-n} \cdot \left( \frac{P \cdot \ln(2)}{1 - 2^{-P}} \right) \quad (3)$$

It must be noted that the inverse signal computed using equation (3), required for the deconvolution of the impulse response, is generated starting from the test signal data, equation (1). Therefore, if a weighting window is applied to the test signal, it will be applied also to the inverse signal. Fixing the higher frequency limit to the Nyquist frequency and spreading the ESS signal over an integer number of

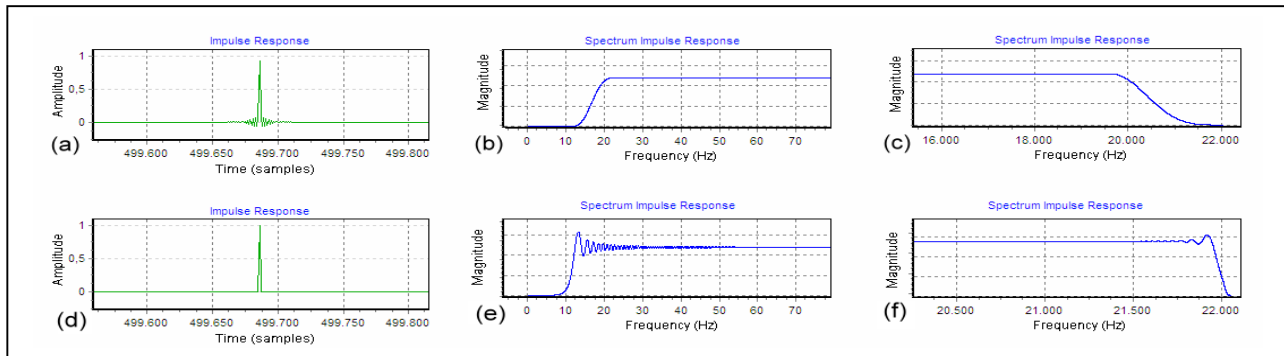


Figure 2. Loopback impulse response taken using an ESS signal: (a) with fade-in and fade-out windows. (b) FFT of (a), initial part. (c) FFT of (a), final part. (d) Without fade-in and fade-out windows. (e) FFT of (d), initial part. (f) FFT of (d), final part.

octaves, the distortion is separated and sorted as much as possible away from the causal part of the impulse response and the signal starts and stops with phase equal to zero, allowing the better results. Some ringing and ripple still remain because the starting frequency of the ESS is not zero (the whole frequency range is not covered). A solution for obtaining a quite smooth spectrum, almost free from ripple, is the use of fade-in and fade-out windows on the generated signal. In order to find the optimal length and shape of these two fading windows, a compromise must be found between two limit situations: i) a smoother frequency response and a worse impulse response, having higher ringing around the initial peak; ii) a frequency response having ripple at the extremes and a better impulse response, with less ringing around the initial peak. Depending on the intended use of the measured impulse response, case i), case

[14], a perfectly clean impulse response is mandatory. Figure 1 (b) shows some samples of a comparison between test measurements performed on a loudspeaker, in ideal conditions, using MLS or the described ESS signal, zooming the amplitude of the plot: the matching is excellent.

Figure 2 (a), (b) and (c), show the application of fade-in and fade-out windows to the ESS in ideal conditions (no A/D-D/A conversion involved). In this case the fade-in window is a one octave long half-left Hanning window and the fade-out window is a 1/6 octave long half-right Hanning window.

The optimal lengths can be found, depending on the target application, as a good compromise between the smoothness of the spectrum extremes (Figures 2(b) and 2(c)) and a low ringing of the impulse response (Figure 2(a)), keeping the frequency response flat on a useful range of interest (including all one-third octave bands from 100 Hz to 10 kHz). For comparison purposes, Figures 2(d), 2(e) and 2(f) show the same computations without the application of fade-in and fade-out windows.

Figure 3 (a) allows to compare the ringing in the time domain, around the peak, measured in a digital loopback configuration (unitary transfer function), using different fade-out window lengths. The

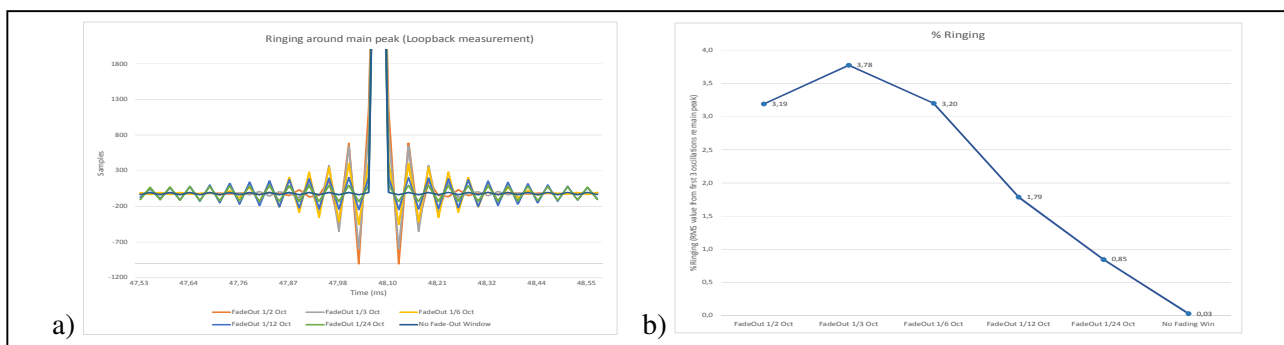


Figure 3. (a) Ringing around the main peak for different Fade-out windows, (b) corresponding percentage ringing.

ii) or a compromise between them could be more desirable. For example, when employing the time subtraction procedure required by CEN/TS 1793-5

ringing percentages shown in (b) have been evaluated as averages of the RMS values of the first 3 oscillations amplitude divided by the main peak amplitude. Without any fading window, the ringing

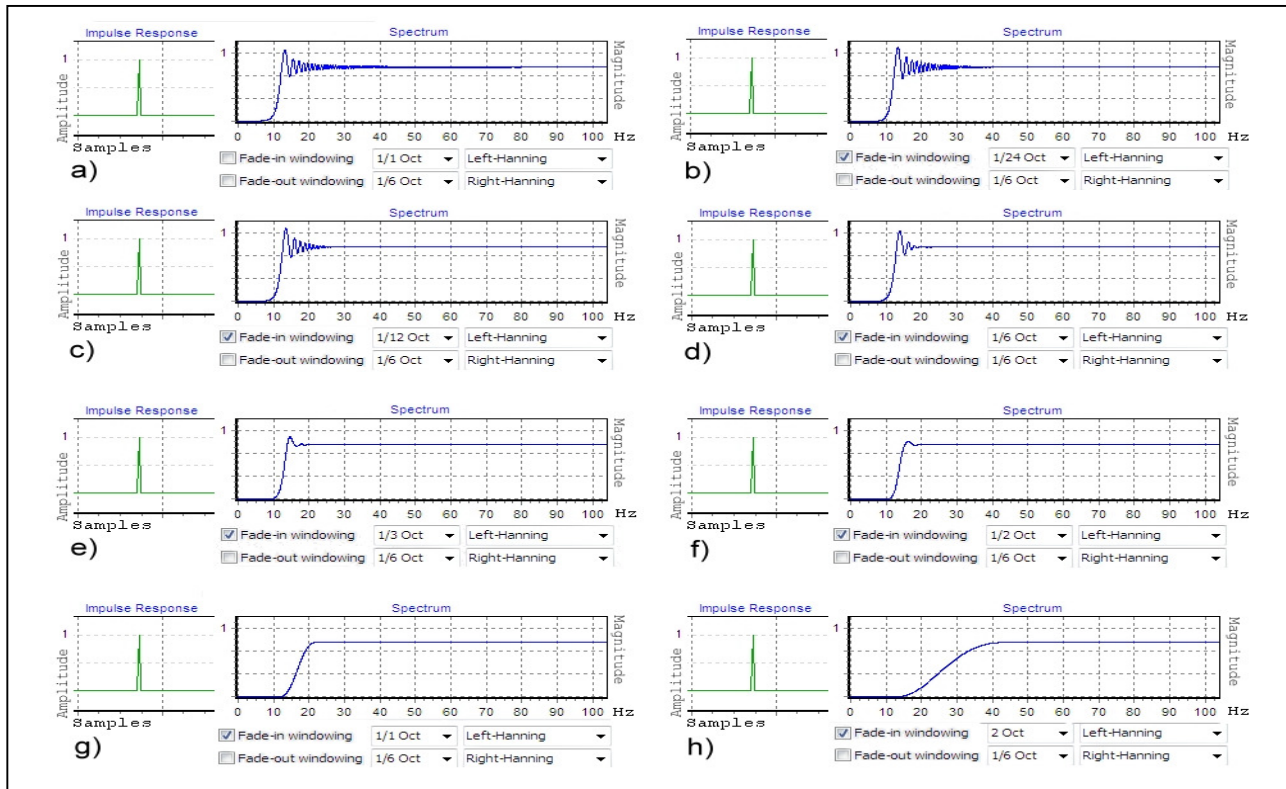


Figure 4. Effect of the length of the fade-in window on the spectrum of the impulse response measured with an ESS signal (fade-out disabled); (a) no fade-in; (b) 1/24 octave fade-in; (c) 1/12 octave fade-in; (d) 1/6 octave fade-in; (e) 1/3 octave fade-in; (f) 1/2 octave fade-in; (g) 1 octave fade-in; (h) 2 octaves fade-in.

lengths of the fade-in and fade-out windows, in order to minimize the ripple on the spectrum. These results have been obtained applying equations 1, 2 and 3 for the generation of the ESS and the impulse response computation. The ESS sequence was 512K samples long and the fade-in and fade-out windows were of the Hanning type (other types of weighting windows do give similar results).

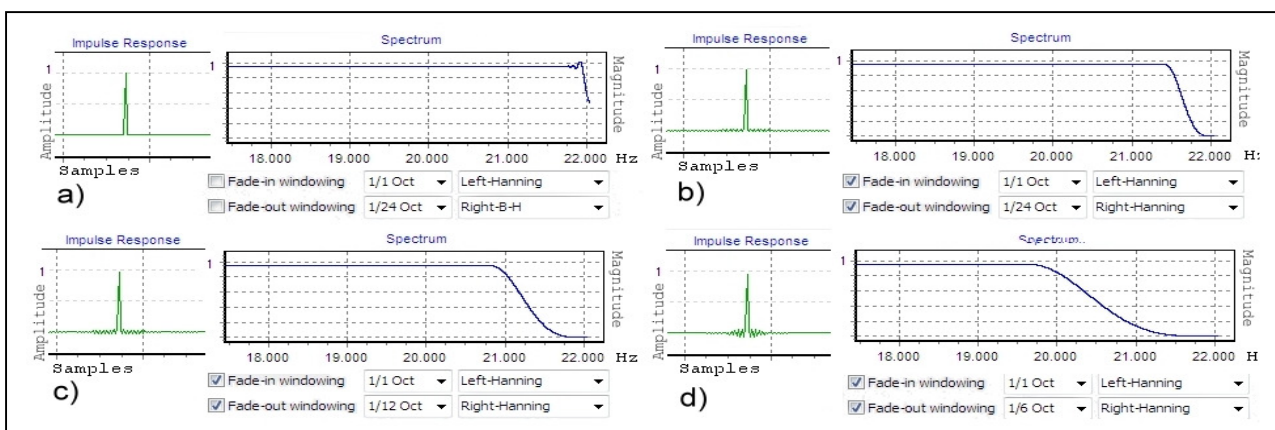


Figure 5. Effect of the length of the fade-out window on the spectrum of the impulse response measured with an ESS signal (fade-in window length fixed to 1 octave). (a) No fade-in and no fade-out; (b) 1/24 octave fade-out; (c) 1/12 octave fade-out; (d) 1/6 octave fade-out;

percentage drops to the negligible value of 0.03% validating the described measurement procedure. Figures 4, 5 and 6 show the effect of different

Measurements were performed using the same soundcard for playing and recording the ESS in real-time, avoiding clock mismatch problems. In Figure 4 the effect of fade-in window application is studied, keeping the fade-out window disabled. The spectrum, obtained from the FFT of the impulse responses, is zoomed in its initial part in order to better analyse the range of frequencies affected by the fade-in windowing.

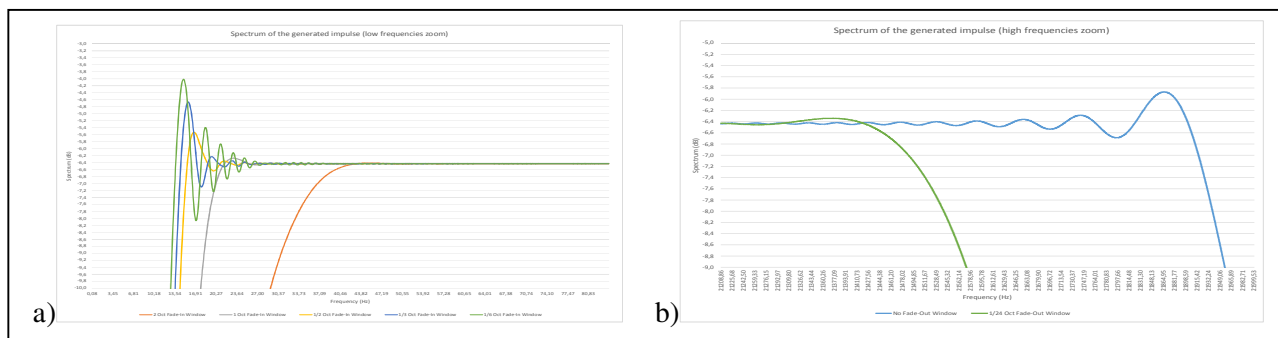


Figure 6. (a) Zoom of the ripple at low spectrum end, for different Fade-in windows; (b) zoom of the ripple at high spectrum end, 1/24 octave fade-out and no windowing.

In (a) the impulse response computed without any fade-in is shown; then in (b), (c), (d), (e), (f), (g) and (h) a 1/24 octave, 1/12 octave, 1/6 octave, 1/3 octave, 1/2 octave, 1 octave or 2 octaves fade-in window is applied, respectively. It can be observed that the fade-in window does not give any time domain ringing effect on the impulse response, but

Table I. Ripple for different fade-in windows length.

Fade-In Window length	2 Oct	1 Oct	1/2	1/3 Oct	1/6 Oct
Max Ripple (dB)	<0,1	0,2	1,1	2,4	4,1

Table II. Ripple for different fade-out windows length.

Fade-Out Window length	No Fading Window	1/24 Oct
Max Ripple (dB)	0,8	<0,2

starting from a minimum length of 1 octave of the weighting window, the magnitude of the frequency response shows a quite smooth rounded shape in the initial part (the ripple disappears). The behaviour of the different fade-in windows lengths can be seen in detail in figure 6 (a); the amplitudes in dB of the first, higher, ripples are shown in Table I. Figure 5 shows the fade-out window application. In all cases shown (except a)), the fade-in window length was fixed at 1 octave. The spectrum, obtained from the FFT of the impulse responses, is zoomed in its final part in order to better analyse the range of frequencies affected by the fade-out windowing. In (a) the impulse response computed without any fade-in and fade-out is shown; in (b), (c), (d) a 1/24 octave, 1/12 octave or 1/6 octave fade-out window was applied, respectively. Figure 6 (b) shows a zoom of the 1/24 octave case and in Table II the ripple values are quantified. Any fade-out window length gives negligible ripple on the

spectrum; without fade-out windowing a residual ripple of about 0.8 dB is found.

#### 4. Example: RI measurement

Figure 7 shows an example of what happens when a reflection index (RI) measurement [14], [15], [16], [17] is performed on a sound absorbing noise barrier, in presence of impulsive noise (traffic noise), using MLS or ESS signals. The measurements were performed at optimal source output level and 30 dB below the optimal output level, without disturbing background noise (as reference), and with the presence of the disturbing

noise, played from another loudspeaker system, at

an average SPL level, measured at the microphone grid, equal, on average, to the measurement signal SPL at the same point. The length of the measurement signals were 512K samples. Measurements at optimal output level are in quite good agreement. Measurements performed in critical conditions (30 dB below optimal level) show large errors, as expected, below 1 kHz. The two measurements obtained with 4 averages MLS and the single shot ESS show both errors on the middle and low frequency bands, with different behaviour: the 4 averages MLS is better at lower frequencies, the ESS is better at the middle frequencies. It is worth noting that, despite the similar amount of errors (in different third octave bands) of the reflection index curves obtained with these two measurements, the corresponding SNR, estimated analysing the impulse responses, would indicate a better expected result for the ESS case (SNR=10.2 dB for the ESS and SNR=5 dB for the

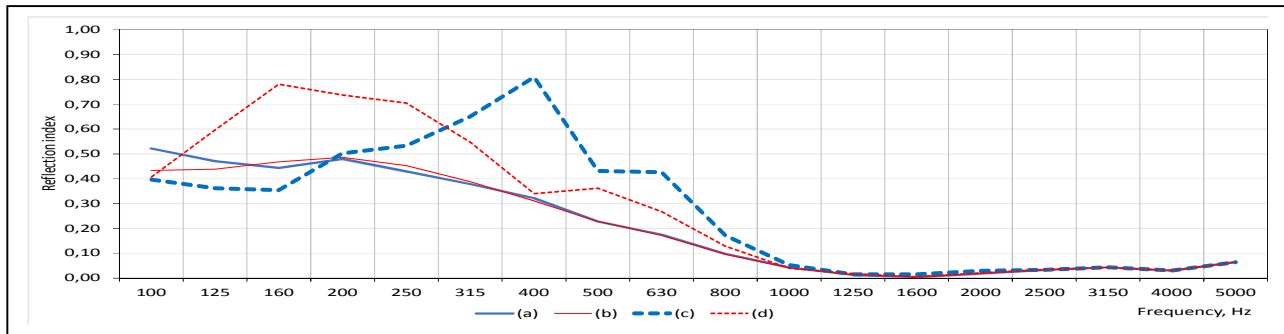


Figure 7. Reflection index measurements on a sound absorbing surface with different signal levels and types (MLS and ESS). Traffic noise disturbance. (a) MLS 4 averages, optimal level. (b) ESS, optimal level. (c) MLS 4 averages, -30 dB. (d) ESS, -30 dB.

4 averages MLS).

## 5. Conclusions

The ESS signal has some advantages over MLS, such as a better signal to noise ratio (SNR) and a robust non-linearity rejection, but some precautions should be used in order to fully exploit its potential. First, impulsive background noise should be avoided; in case of its occurrence, taking a new measurement is the preferred option. Second, the generation of the ESS should be phase controlled and a data windowing targeted to the specific application of the measured impulse response should be applied, in order to optimize the results and avoid possible computation errors.

Findings from this work suggest that: i) the shape of the data window is not critical, provided it is smooth enough; ii) the fade-in window should be 1-octave wide, while the fade-out window should be 1/24 or 1/12-octave wide. By using a shorter fade-out window, the ringing around the first peak of the impulse response can be avoided, if required by a specific application.

## References

- [1] M.R. Schröder: Integrated-impulse method measuring sound decay without using impulses. *J. Acoust. Soc. Am.*, 66(2) (1979) 497-500.
- [2] D. D. Rife, J. Vanderkooy: Transfer-function measurement with maximum length sequences. *J. Audio Eng. Soc.*, 37(6) (1989) 419-444.
- [3] G. Stan, J.J. Embrechts, D. Archambeau: Comparison of Different Impulse Response Measurement Techniques. *J. Audio Eng. Soc.*, 5(4) (2002) 249.
- [4] S. Müller, P. Massarani: Transfer-Function Measurement with sweeps. Director's Cut including previously unreleased material and some corrections. Originally in *J. Audio Eng. Soc.*, 49 (2001) 443-471.
- [5] A. Farina: Simultaneous Measurement of Impulse Response and Distortion with a Swept-Sine Technique. 108th Convention of the Audio Engineering Society, paper 5093, (2000 Feb.).
- [6] A. Farina: Advancements in Impulse Response Measurements by Sine Sweeps. 122nd Convention of the Audio Engineering Society, paper 7121, (2007 May).
- [7] A. Torras-Rosell, F. Jacobsen: A New Interpretation of Distortion Artifacts in Sweep Measurements. *J. Audio Eng. Soc.*, 59 (2011) 283-289.
- [8] D. Ćirić: Comparison of influence of distortion in MLS and Sine Sweep technique. 19th International Congress on Acoustics, paper RBA-07-020, (2007 September)
- [9] J. Kemp, H. Primack: Impulse Response Measurement of Nonlinear Systems: Properties of Existing Techniques and Wide Noise Sequences. *J. Audio Eng. Soc.*, 59(2011) 953-963.
- [10] P. Dietrich, B. Masiero, M. Vorländer: On the Optimization of the Multiple Exponential Sweep Method. *J. Audio Eng. Soc.*, 61(2013) 113-124.
- [11] M. Guski, M. Vorländer: Comparison of Noise Compensation Methods for Room Acoustic Impulse Response Evaluations. *Acta Acustica united with Acustica*, 100(2014), 320-327(8).
- [12] A. Novák, L. Simon, F. Kadlec, P. Lotton: Nonlinear system identification using exponential swept-sine signal. *IEEE Transactions on Instrumentation and Measurement* 59(8) (2010), 2220-2229.
- [13] K. Vetter, S. di Rosario: ExpoChirpToolbox: a Pure Data implementation of ESS impulse response measurement. Pure Data Convention 2011, Weimer-Berlin (2011).
- [14] CEN/TS 1793-5:2003, "Road traffic noise reducing devices - Test method for determining the acoustic performance - Part 5: Intrinsic characteristics - In situ values of airborne sound reflection and airborne sound insulation".
- [15] EN 1793-6:2012: Road traffic noise reducing devices - Test method for determining the acoustic performance - Part 6: Intrinsic characteristics - In situ values of airborne sound insulation under direct sound field conditions.
- [16] M. Garai, P. Guidorzi: In situ measurements of the intrinsic characteristics of the acoustic barriers installed along a new high speed railway line. *Noise Control Eng. J.*, 56 (2008) 342-355.
- [17] M. Garai, E. Schoen, G. Behler, B. Bragado, M. Chudalla, M. Conter, J. Defrance, P. Demizieux, C. Glorieux, P. Guidorzi: Repeatability and reproducibility of in situ measurements of sound reflection and airborne sound insulation index of noise barriers, *Acta Acustica united with Acustica*, 100 (2014) 1186-1201.